

BUCKLING OF SHALLOW SHELLS OF DOUBLE CURVATURE STIFFENED BY RIBS FROM THE OUTSIDE

Alexey Semenov

Saint Petersburg State University of Architecture and Civil Engineering, Saint Petersburg,
190005, Russian Federation
e-mail: sw.semenov@gmail.com

Abstract

The results of a computational experiment on the analysis of the effectiveness of placing stiffeners on the outer side of the shell structure are presented. The calculations were carried out on the basis of a geometrically nonlinear mathematical model that takes into account transverse shears and orthotropy of the material. The calculation algorithm is based on the Ritz method and the method of continuing the solution with respect to the best parameter. To take into account stiffeners, the refined discrete method, proposed by the author earlier, is used. Shallow shells of double curvature are analyzed. The structures are made of steel and are simply supported, the stiffening ribs are arranged orthogonally. The values of critical buckling loads are presented. The effectiveness of the location of the stiffeners on the outer side of the shell structure is shown. It is revealed that the location of the ribs on the outside increases the value of the critical buckling load.

Keywords: stiffened shells, buckling, outside ribs, Ritz method, mathematical model.

1. Introduction

The study of the process of deformation of shell structures is essential for various industries, including aircraft, building, shipbuilding, rocket science, and others (Al-Hashimi et al. (2009), Efimtsov and Lazarev (2009), Garcia and Ramos (2021), Sun et al. (2013), Uematsu et al. (2001), Ghasemi et al. (2021), Verwimp et al. (2015), Yu and Li (2016)). In construction, such structures are often used, for example, to cover large-span structures.

The main requirement for shell-coatings of building structures is to ensure safe and long-term reliability of the structure at given levels of loads. At the same time, it is also important to reduce the material consumption of shell structures. Coating shells of building structures are made from various materials: reinforced concrete, steel, composite materials, some of which can be considered as orthotropic materials.

Ghasemi et al. (2021) developed a new multi-step optimization method to predict the optimal fiber orientation in GFRP composite shells. Some experiments are conducted to evaluate the critical buckling pressure in GFRP specimens, and the obtained analytical results are verified through comparison with experimental ones.

When calculating thin-walled shells, it is important to take into account the presence of reinforcement with stiffeners (Solovei et al. (2015), Dung and Nam (2014), Less and Abramovich (2012), Qu et al. (2013), Wang et al. (2016)), since this enables significant increase in the value of the critical load, redistribution of dangerous stresses, and thereby improvement of the performance of the structure.

In Yu and Li (2016) the generalized similitude requirements and the scaling law of orthogonally stiffened cylindrical panels and shells for buckling and free vibration are derived by applying the similitude transformation to the total energy of the structural system.

Structures reinforced with stiffeners are much more difficult to investigate than structures of constant thickness. There are several approaches to the introduction of stiffeners. For example, in Kidane et al. (2003) and Jaunky et al. (1996), a discrete approach is singled out, which can be found, for example, in Qu et al. (2013), Amiro and Zarutskii (1983), Huang and Qiao (2020), Kholmuradov and Ismoilov (2020), Lee and Kim (1998), Mustafa and Ali (1989), Sadeghifar et al. (2011), Talebitooti et al. (2010), Wang et al. (1997), Wang and Hsu (1985) and Zhao et al. (2002), as well as an approach with stiffness smearing (Efimtsov and Lazarev (2009), Jaunky et al. (1996), Bich et al. (2013), Buragohain and Velmurugan (2009), Srinivasan and Krishnan (1989), Totaro (2016), Tu and Loi (2016), etc.).

In Qu et al. (2013), free vibration characteristics of shell combinations with ring stiffeners are investigated by using a modified variational method. Reissner–Naghdi’s thin shell theory in conjunction with a multilevel partition technique, viz., stiffened shell combination, shell component and shell segment, is employed to formulate the theoretical model.

Reviews on stiffened shells and the application of stiffening smearing methods can be found in significant papers (Wang et al. (2016), Jaunky et al. (1996), Sadeghifar et al. (2011), Buragohain and Velmurugan (2009), Jones (1968), Ren et al. (2014)).

Ren et al. (2014) performed buckling experiment on an advanced grid stiffened structure to validate the efficiency of different modeling methods. Based on the comparison, the characteristics of different methods are independently evaluated.

Earlier in Semenov (2021) and Karpov and Semenov (2020) the authors proposed a refined discrete method for calculating stiffening structures. In these papers, the application is extended to the class of shallow shells of double curvature, stiffened with stiffeners from the outside.

2. Theory and Methods

2.1 Fundamental relations

For the Timoshenko (Mindlin – Reissner) model, displacements in a layer located at a distance z from the middle surface will take the form

$$U^z = U + z\Psi_x, \quad V^z = V + z\Psi_y, \quad W^z = W \quad (1)$$

where U , V , W – displacements of points of the middle surface along the local shell axes x , y , z respectively; Ψ_x , Ψ_y – angles of rotation of the normal in the planes xOz , yOz .

Geometric relations in the middle surface of the shell, taking into account the geometric nonlinearity, are presented as follows:

$$\begin{aligned}
\varepsilon_x &= \frac{1}{A} \frac{\partial U}{\partial x} + \frac{1}{AB} V \frac{\partial A}{\partial y} - k_x W + \frac{1}{2} \theta_1^2, \\
\varepsilon_y &= \frac{1}{B} \frac{\partial V}{\partial y} + \frac{1}{AB} U \frac{\partial B}{\partial x} - k_y W + \frac{1}{2} \theta_2^2, \\
\gamma_{xy} &= \frac{1}{A} \frac{\partial V}{\partial x} + \frac{1}{B} \frac{\partial U}{\partial y} - \frac{1}{AB} U \frac{\partial A}{\partial y} - \frac{1}{AB} V \frac{\partial B}{\partial x} + \theta_1 \theta_2, \\
\theta_1 &= -\left(\frac{1}{A} \frac{\partial W}{\partial x} + k_x U \right), \quad \theta_2 = -\left(\frac{1}{B} \frac{\partial W}{\partial y} + k_y V \right), \quad k_x = \frac{1}{R_1}, \quad k_y = \frac{1}{R_2},
\end{aligned} \tag{2}$$

where $\varepsilon_x, \varepsilon_y$ – strains along coordinates x, y of middle surface; $\gamma_{xy}, \gamma_{xz}, \gamma_{yz}$ – shear strains in xOy, xOz, yOz ; A, B are Lamé parameters; k_x, k_y are the primary curvatures of the shell along the x and y axes; R_1, R_2 are the principal curvature radii characterizing the geometry of the shell. Geometric relations for a layer, spaced at z from the middle surface are expressed as follows:

$$\varepsilon_x^z = \varepsilon_x + z\chi_1, \quad \varepsilon_y^z = \varepsilon_y + z\chi_2, \quad \gamma_{xy}^z = \gamma_{xy} + 2z\chi_{12}, \tag{3}$$

and the curvature functions χ_1, χ_2 and torsion function χ_{12} are:

$$\begin{aligned}
\chi_1 &= \frac{1}{A} \frac{\partial \Psi_x}{\partial x} + \frac{1}{AB} \frac{\partial A}{\partial y} \Psi_y, \quad \chi_2 = \frac{1}{B} \frac{\partial \Psi_y}{\partial y} + \frac{1}{AB} \frac{\partial B}{\partial x} \Psi_x, \\
\chi_{12} &= \frac{1}{2} \left[\frac{1}{A} \frac{\partial \Psi_y}{\partial x} + \frac{1}{B} \frac{\partial \Psi_x}{\partial y} - \frac{1}{AB} \left(\frac{\partial A}{\partial y} \Psi_x + \frac{\partial B}{\partial x} \Psi_y \right) \right].
\end{aligned} \tag{4}$$

The shape of the shell structure is specified through the Lamé parameters and the values of the radii of the main curvatures of the shell.

In order to find stresses, stress-strain relations are used:

$$\begin{aligned}
\sigma_x &= \frac{E_1}{1 - \mu_{12}\mu_{21}} \left[\varepsilon_x + \mu_{21}\varepsilon_y + z(\chi_1 + \mu_{21}\chi_2) \right], \\
\sigma_y &= \frac{E_2}{1 - \mu_{12}\mu_{21}} \left[\varepsilon_y + \mu_{12}\varepsilon_x + z(\chi_2 + \mu_{12}\chi_1) \right], \\
\tau_{xy} &= G_{12} \left[\gamma_{xy} + 2z\chi_{12} \right], \quad \tau_{xz} = G_{13} k f(z) (\Psi_x - \theta_1), \quad \tau_{yz} = G_{23} k f(z) (\Psi_y - \theta_2).
\end{aligned} \tag{5}$$

Here, $E_1, E_2, \mu_{12}, \mu_{21}$ are the elastic moduli and Poisson coefficients of the shell material; G_{12}, G_{13}, G_{23} are the shear moduli in the xOy, xOz, yOz planes, respectively; $f(z)$ is a function characterizing the distribution of shear strains γ_{xz}, γ_{yz} along the thickness of the shell; and k is a numerical coefficient:

$$f(z) = 6 \left(\frac{1}{4} - \frac{z^2}{h^2} \right), \quad k = \frac{5}{6}$$

For shells, stiffened by ribs, it is convenient to write separately the parts of the model related to the skin, and separately the parts related to the stiffeners.

First, the expressions for the forces and moments that occur in the skin (superscript “0”) are considered – they are found by integrating stresses (5) by z from $-h/2$ to $h/2$:

$$\begin{aligned} N_x^0 &= G_1^0 h (\varepsilon_x + \mu_{21} \varepsilon_y), \quad N_y^0 = G_2^0 h (\varepsilon_y + \mu_{12} \varepsilon_x), \quad N_{xy}^0 = N_{yx}^0 = G_{12}^0 h \gamma_{xy}, \\ M_x^0 &= G_1^0 \frac{h^3}{12} (\chi_1 + \mu_{21} \chi_2), \quad M_y^0 = G_2^0 \frac{h^3}{12} (\chi_2 + \mu_{12} \chi_1), \quad M_{xy}^0 = M_{yx}^0 = 2G_{12}^0 \frac{h^3}{12} \chi_{12}, \\ Q_x^0 &= kG_{13}^0 h (\Psi_x - \theta_1), \quad Q_y^0 = kG_{23}^0 h (\Psi_y - \theta_2), \end{aligned}$$

where

$$G_1^0 = \frac{E_1}{1 - \mu_{12} \mu_{21}}, \quad G_2^0 = \frac{E_2}{1 - \mu_{12} \mu_{21}}.$$

As a basis for the mathematical model of deformation of the shell structure, it takes the functional of the total potential energy of deformation (the Lagrange functional). Models built using the functional were also considered by many authors (Qu et al. (2013), Jaunky et al. (1996), Lee and Kim (1998), Mustafa and Ali (1989), Talebitooti et al. (2010), etc.).

Represent the functional as the difference between the potential energy of the system and the work of external forces

$$E_s = E_s^0 + E_p^R = E_p^0 + E_p^R - A, \quad (6)$$

where E_s^0 – component of the functional related to the skin; E_p^R – potential deformation energy of the system related to stiffeners; E_p^0 – potential deformation energy of the system related to the skin; A (alfa) – work of external forces.

Part of the functional related to the skin:

$$E_s^0 = \frac{1}{2} \int_{a_1}^a \int_0^b \left[N_x^0 \varepsilon_x + N_y^0 \varepsilon_y + \frac{1}{2} (N_{xy}^0 + N_{yx}^0) \gamma_{xy} + M_x^0 \chi_1 + M_y^0 \chi_2 + (M_{xy}^0 + M_{yx}^0) \chi_{12} \right. \\ \left. + Q_x^0 (\Psi_x - \theta_1) + Q_y^0 (\Psi_y - \theta_2) - 2(P_x U + P_y V + qW) \right] AB dx dy, \quad (7)$$

and E_p^R part of the functional related to stiffeners

$$E_p^R = \frac{1}{2} \int_{a_1}^a \int_0^b \left[N_x^R \varepsilon_x + N_y^R \varepsilon_y + \frac{1}{2} (N_{xy}^R + N_{yx}^R) \gamma_{xy} + M_x^R \chi_1 + M_y^R \chi_2 \right. \\ \left. + (M_{xy}^R + M_{yx}^R) \chi_{12} + Q_x^R (\Psi_x - \theta_1) + Q_y^R (\Psi_y - \theta_2) \right] AB dx dy. \quad (8)$$

As a rule, if an external load is applied along the normal to the surface of the shell, then $P_x = P_{xsv}$, $P_y = P_{ysv}$ (self-weight load components), and its transverse component can be given as $q = q_0 + q_{sv}$, where q_0 – applied lateral load, MPa; q_{sv} – transverse load component due to shell self-weight, MPa.

In accordance with the refined discrete method for taking into account stiffeners, the forces and moments acting in the ribs can be written as (Karpov and Semenov, 2020):

$$\begin{aligned}
N_x^R &= G_1^R \left[\bar{F}_x (\varepsilon_x + \mu_{21} \varepsilon_y) + \bar{S}_x (\chi_1 + \mu_{21} \chi_2) \right], M_x^R = G_1^R \left[\bar{S}_x (\varepsilon_x + \mu_{21} \varepsilon_y) + \bar{J}_x (\chi_1 + \mu_{21} \chi_2) \right], \\
N_y^R &= G_2^R \left[\bar{F}_y (\varepsilon_y + \mu_{12} \varepsilon_x) + \bar{S}_y (\chi_2 + \mu_{12} \chi_1) \right], M_y^R = G_2^R \left[\bar{S}_y (\varepsilon_y + \mu_{12} \varepsilon_x) + \bar{J}_y (\chi_2 + \mu_{12} \chi_1) \right], \\
N_{xy}^R &= G_{12}^R \left[\bar{F}_{xy} \gamma_{xy} + 2 \bar{S}_{xy} \chi_{12} \right], M_{xy}^R = G_{12}^R \left[\bar{S}_{xy} \gamma_{xy} + \bar{J}_{xy} \chi_{12} \right], \\
Q_x^R &= G_{13}^R k \bar{F}_x (\Psi_x - \theta_1), Q_y^R = G_{23}^R k \bar{F}_y (\Psi_y - \theta_2), \\
G_1^R &= \frac{E_1}{1 - \mu_{12} \mu_{21}}, G_2^R = \frac{E_2}{1 - \mu_{12} \mu_{21}}.
\end{aligned} \tag{9}$$

Here

$$\begin{aligned}
\bar{F}_x &= \sum_{i=1}^n F^i \bar{\delta}(y - y_i) + r_a \left[\sum_{j=1}^m F^j \bar{\delta}(x - x_j) - \sum_{i=1}^n \sum_{j=1}^m F^{ij} \bar{\delta}(x - x_j) \bar{\delta}(y - y_i) \right], \\
\bar{F}_y &= \sum_{j=1}^m F^j \bar{\delta}(x - x_j) + r_b \left[\sum_{i=1}^n F^i \bar{\delta}(y - y_i) - \sum_{i=1}^n \sum_{j=1}^m F^{ij} \bar{\delta}(x - x_j) \bar{\delta}(y - y_i) \right], \\
\bar{S}_x &= \sum_{i=1}^n S^i \bar{\delta}(y - y_i) + r_a \left[\sum_{j=1}^m S^j \bar{\delta}(x - x_j) - \sum_{i=1}^n \sum_{j=1}^m S^{ij} \bar{\delta}(x - x_j) \bar{\delta}(y - y_i) \right], \\
\bar{S}_y &= \sum_{j=1}^m S^j \bar{\delta}(x - x_j) + r_b \left[\sum_{i=1}^n S^i \bar{\delta}(y - y_i) - \sum_{i=1}^n \sum_{j=1}^m S^{ij} \bar{\delta}(x - x_j) \bar{\delta}(y - y_i) \right], \\
\bar{J}_x &= \sum_{i=1}^n J^i \bar{\delta}(y - y_i) + r_a \left[\sum_{j=1}^m J^j \bar{\delta}(x - x_j) - \sum_{i=1}^n \sum_{j=1}^m J^{ij} \bar{\delta}(x - x_j) \bar{\delta}(y - y_i) \right], \\
\bar{J}_y &= \sum_{j=1}^m J^j \bar{\delta}(x - x_j) + r_b \left[\sum_{i=1}^n J^i \bar{\delta}(y - y_i) - \sum_{i=1}^n \sum_{j=1}^m J^{ij} \bar{\delta}(x - x_j) \bar{\delta}(y - y_i) \right], \\
\bar{F}_{xy} &= \frac{1}{2} (\bar{F}_x + \bar{F}_y) = \frac{1}{2} \sum_{i=1}^n F^i (1 + r_b) \bar{\delta}(y - y_i) + \frac{1}{2} \sum_{j=1}^m F^j (1 + r_a) \bar{\delta}(x - x_j) - \\
&\quad - \sum_{i=1}^n \sum_{j=1}^m F^{ij} r_{ab} \bar{\delta}(x - x_j) \bar{\delta}(y - y_i), \\
\bar{S}_{xy} &= \frac{1}{2} (\bar{S}_x + \bar{S}_y) = \frac{1}{2} \sum_{i=1}^n S^i (1 + r_b) \bar{\delta}(y - y_i) + \frac{1}{2} \sum_{j=1}^m S^j (1 + r_a) \bar{\delta}(x - x_j) - \\
&\quad - \sum_{i=1}^n \sum_{j=1}^m S^{ij} r_{ab} \bar{\delta}(x - x_j) \bar{\delta}(y - y_i), \\
\bar{J}_{xy} &= \frac{1}{2} (\bar{J}_x + \bar{J}_y) = \frac{1}{2} \sum_{i=1}^n J^i (1 + r_b) \bar{\delta}(y - y_i) + \frac{1}{2} \sum_{j=1}^m J^j (1 + r_a) \bar{\delta}(x - x_j) - \\
&\quad - \sum_{i=1}^n \sum_{j=1}^m J^{ij} r_{ab} \bar{\delta}(x - x_j) \bar{\delta}(y - y_i),
\end{aligned} \tag{10}$$

where

$$F^i = h^i, \quad F^j = h^j, \quad F^{ij} = h^{ij}, \quad S^i = h^i (h + h^i) / 2, \quad S^j = h^j (h + h^j) / 2, \quad S^{ij} = h^{ij} (h + h^{ij}) / 2,$$

$$J^i = 0.25h^2h^i + 0.5h(h^i)^2 + \frac{1}{3}(h^i)^3,$$

$$J^j = 0.25h^2h^j + 0.5h(h^j)^2 + \frac{1}{3}(h^j)^3, \quad J^{ij} = 0.25h^2h^{ij} + 0.5h(h^{ij})^2 + \frac{1}{3}(h^{ij})^3$$

and

$$r_a = \frac{r_j}{(a - a_1)A}, \quad r_b = \frac{r_i}{bB}, \quad r_{ab} = \frac{r_a + r_b}{2}. \quad (11)$$

Here h^i, h^j – stiffeners height; superscripts i and j indicates the number of the stiffener located parallel to the axis x and y respectively; n, m – ribs amount; $h^{ij} = \min\{h^i, h^j\}$, that is, the common part of the intersection of the stiffeners; $\bar{\delta}(x - x_j)$ and $\bar{\delta}(y - y_i)$ – unit column functions, which are the differences of two unit functions $\bar{\delta}(x - x_j) = U(x - a_j) - U(x - b_j)$; $\bar{\delta}(y - y_i) = U(y - c_i) - U(y - d_i)$, where $a_j = x_j - r_j / (2A)$, $b_j = x_j + r_j / (2A)$, $c_i = y_i - r_i / (2B)$, $d_i = y_i + r_i / (2B)$, r_i, r_j – width of stiffeners.

In order to place the stiffeners on the outer side of the skin, it is necessary in Eq. (10) for the variables $\bar{S}_x, \bar{S}_y, \bar{S}_{xy}$ to change the sign to the opposite one (i.e. to “-”).

2.2 Methods

In this paper, for the study of shell structures, it is proposed to use an algorithm based on the Ritz method and the method of continuing the solution with respect to the best parameter (Semenov (2016)).

According to this algorithm, the Ritz method is applied to the functional to reduce the variational problem to a system of nonlinear algebraic equations. To do this, the desired functions are represented in the form:

$$\begin{aligned} U &= U(x, y) = \sum_{k=1}^{\sqrt{N}} \sum_{l=1}^{\sqrt{N}} U_{kl} X_1^k Y_1^l, & V &= V(x, y) = \sum_{k=1}^{\sqrt{N}} \sum_{l=1}^{\sqrt{N}} V_{kl} X_2^k Y_2^l, \\ W &= W(x, y) = \sum_{k=1}^{\sqrt{N}} \sum_{l=1}^{\sqrt{N}} W_{kl} X_3^k Y_3^l, & \Psi_x &= \Psi_x(x, y) = \sum_{k=1}^{\sqrt{N}} \sum_{l=1}^{\sqrt{N}} P S_{kl} X_4^k Y_4^l, \\ \Psi_y &= \Psi_y(x, y) = \sum_{k=1}^{\sqrt{N}} \sum_{l=1}^{\sqrt{N}} P N_{kl} X_5^k Y_5^l, \end{aligned} \quad (12)$$

where $U_{kl} - P N_{kl}$ – unknown numeric parameters. Substituting Eq. (12) into functional Eq. (7), (8), derivatives can be found with respect to the unknown numerical parameters $U_{kl} - P N_{kl}$. Thus, a system of nonlinear algebraic equations is obtained.

To solve this system, the method of continuing the solution with respect to the best parameter is used.

All calculations are carried out in dimensionless parameters; however, all formulas and results are given in dimensional form.

3. Numerical Results

The applicability of the method described above for introducing stiffeners is demonstrated by the example of calculating flat shells of double curvature (Table 1) made of steel with parameters $E_1 = E_2 = 2.1 \cdot 10^5$ MPa, $\mu_{12} = \mu_{21} = 0.3$. The shells are square in plan, simply supported along the contour and are under the action of a uniformly distributed transverse load q directed along the normal to the surface.

The shells are stiffened by an orthogonal grid of ribs distributed evenly over the structure. Ribs width $r^j = r^i = 2h$, ribs height $h^j = h^i = 3h$. The distance between the ribs is denoted x_r , and the outside ribs will be located from the contour of the structure at a distance $0.5x_r$.

h , m	a , m	b , m	R_1 , m	R_2 , m
0.09	18	18	45.27	45.27

Table 1. Geometrical parameters of shells.

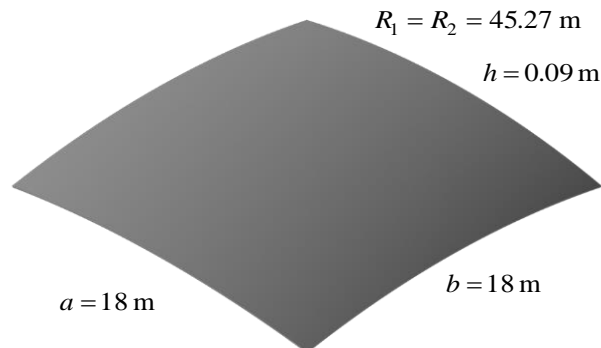


Fig. 1. Considered shallow shells of double curvature.

In Eq. (12) takes $N = 16$.

The number of stiffeners will be taken the same in both directions, increasing it by 4 for each new version of the grid.

Table 2 shows the values of critical buckling loads for different stiffening options, obtained using the refined discrete method of considering stiffeners.

As can be seen from the presented data, the reinforcement of the structure with stiffeners from the outside is effective. Fig. 2 shows graphs of the corresponding dependencies "load –

deflection”. The red curve W_c in the diagrams depicts the deflection in the center of a structure ($x = (a_1 + a)/2, y = b/2$), and the blue curve W_4 the deflection in the quadrant of a structure ($x = (3a_1 + a)/4, y = b/4$).

Stiffening scheme	Critical buckling load q_{cr} , MPa			
	0×0	4×4	8×8	12×12
Ribs on the inner side	0.6238	1.1411	2.5078	3.0508
Ribs on the outer side		1.9087	3.2679	3.2115

Table 2. Critical buckling loads for the considered shell when placing stiffeners on the inside or outside.

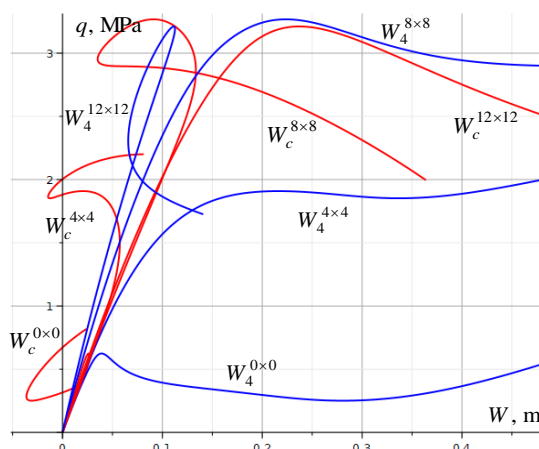


Fig. 2. Results for the considered shell with stiffeners located on the outside.

From Fig. 2 it can be seen that an increase in the number of stiffening elements at a certain moment changes the form of the deformation process: before the increase in the grid of stiffeners to 12x12, the formation of loops in the “load – deflection” graph at the central point was specific, which indicates the formation of dents and local buckling. With a grid of stiffeners 12x12, the value of the critical buckling load is slightly reduced; however, this is a compensating effect from the stabilization of the deformation process and the disappearance of local buckling in the central part of the structure.

The proposed method was verified for shells stiffening with ribs on the inside (due to the fact that the author could not find experimental results for problems in an absolutely identical formulation in known sources).

In their publication, Klimanov and Timashev (1985) present results of experiments conducted at the Ural Research Center of the USSR Academy of Sciences to study the buckling of plexiglass shells. The authors tested 18 samples of square shallow doubly curved shells with parameters $h = 0.001$ m, $a = b = 0.604$ m, $R_1 = R_2 = 1.51$ m (material: plexiglass with parameters $E = 0.0331 \cdot 10^5$ MPa, $\mu = 0.354$; parameters of stiffeners: $n = m = 9$, $h^i = h^j = 0.0033$ m, $r = 0.0092$ m). The resulting buckling load values q_{cr} ranged from

$0.411 \cdot 10^{-2}$ MPa to $0.703 \cdot 10^{-2}$ MPa. After mathematical processing of the experimental data, the resultant value of the critical load was calculated to be $q_{cr} = 0.503 \cdot 10^{-2}$ MPa.

Analysis for this version of the structure using the refined discrete method, mathematical model and algorithm, described in this paper, yielded the critical buckling load $q_{cr} = 0.551 \cdot 10^{-2}$ MPa which is in good agreement with the experimental results.

Verification of the kind of the resulting curves can be partially compared with the work of Wang (2007), where orthotropic shallow shells of double curvature, square in plan and simply supported on the contour are investigated. In the base of the algorithm, it is proposed to use DQM (Differential quadrature method). Parameters of the shell: $a = b = 0.2$ m, $R_1 = 5$ m, $R_2 = 3.33$ m, $h = 0.00022$ m, $E_1 = 0.2 \cdot 10^5$ MPa, $E_2 = 0.4 \cdot 10^5$ MPa, $\mu_{12} = 0.1$, $G_{12} = 0.1 \cdot 10^5$ MPa. It should be noted that the model presented in Wang (2007), in contrast to the proposed model, does not include the effect of transverse shears. The “load q – deflection W ” graph are shown in Fig. 3.

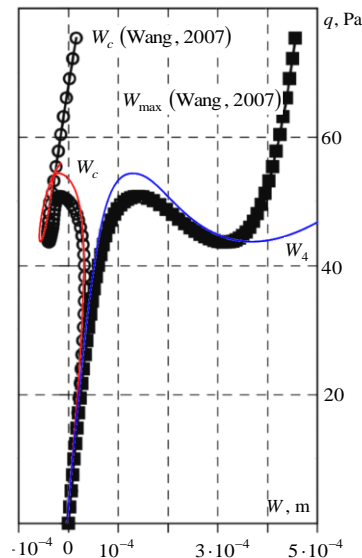


Fig. 3. Verification of the proposed methodology (comparison with Wang (2007)).

4. Conclusions

The author extended the previously proposed refined discrete method for accounting for stiffeners to the class of shallow shells of double curvature, reinforced with stiffeners from the outside. The bottom line is to add different reduction factors along different coordinate axes. For stiffeners directed perpendicular to the considered direction, a reduction factor is introduced equal to the ratio of the width of the ribs in this direction to the linear size of the shell in the considered direction.

Analysis was made for the buckling of steel shallow shells of double curvature, stiffening by ribs from the outside or from the inside. Comparison of results is carried out. It was found that

the location of the ribs on the outside increases the value of the critical load of buckling, and can have an effect of up to 40 %, decreasing with an increase in the number of stiffening elements.

References

- Al-Hashimi H, Seibi AC and Molki A (2009). Experimental Study and Numerical Simulation of Domes Under Wind Load. *Proceedings of the ASME 2009 Pressure Vessels and Piping Division Conference*. Prague, Czech Republic: ASME, 519–528.
- Amiro IY and Zarutskii VA (1983). Stability of ribbed shells. *Soviet Applied Mechanics* 19(11): 925–940.
- Bich DH, Dung DV and Nam VH (2013). Nonlinear dynamic analysis of eccentrically stiffened imperfect functionally graded doubly curved thin shallow shells. *Composite Structures* 96: 384–395.
- Buragohain M and Velmurugan R (2009). Buckling Analysis of Composite Hexagonal Lattice Cylindrical Shell using Smeared Stiffener Model. *Defence Science Journal* 59(3): 230–238.
- Dung DV and Nam VH (2014). An analytical approach to analyze nonlinear dynamic response of eccentrically stiffened functionally graded circular cylindrical shells subjected to time dependent axial compression and external pressure. Part 2: Numerical results and discussion. *Vietnam Journal of Mechanics* 36(4): 255–265.
- Efimtov BM and Lazarev LA (2009). Forced vibrations of plates and cylindrical shells with regular orthogonal system of stiffeners. *Journal of Sound and Vibration* 327(1–2): 41–54.
- Garcia FG and Ramos R (2021). Design charts for the local buckling analysis of integrally web-stiffened panels with filleted junctions subjected to uniaxial compressive loads. *Thin-Walled Structures* 108632.
- Ghasemi AR, Tabatabaeian A, Hajmohammad MH and Tornabene F (2021). Multi-step buckling optimization analysis of stiffened and unstiffened polymer matrix composite shells: A new experimentally validated method. *Composite Structures* 273: 114280.
- Huang S and Qiao P (2020). A new semi-analytical method for nonlinear stability analysis of stiffened laminated composite doubly-curved shallow shells. *Composite Structures* 251: 112526.
- Jaunky N, Knight NF and Ambur DR (1996). Formulation of an improved smeared stiffener theory for buckling analysis of grid-stiffened composite panels. *Composites Part B: Engineering* 27(5): 519–526.
- Jones RM (1968). Buckling of circular cylindrical shells with multiple orthotropic layers and eccentric stiffeners. *AIAA Journal* 6(12): 2301–2305.
- Karpov VV and Semenov AA (2020) Refined model of stiffened shells. *International Journal of Solids and Structures* 199: 43–56.
- Khalmuradov RI and Ismoilov EA (2020). Nonlinear vibrations of a circular plate reinforced by ribs. *IOP Conference Series: Earth and Environmental Science* 614: 012071.
- Kidane S, Li G, Helms J, Pang S-S and Woldeesenbet E (2003). Buckling load analysis of grid stiffened composite cylinders. *Composites Part B: Engineering* 34(1): 1–9.
- Klimanov VI, Timashev SA (1985). *Nonlinear Problems of Reinforced Shells*. USC of USSR Academy of Sciences, Sverdlovsk. (in Russian)
- Lee Y-S and Kim Y-W (1998). Vibration analysis of rotating composite cylindrical shells with orthogonal stiffeners. *Computers & Structures* 69(2): 271–281.
- Less H and Abramovich H (2012). Dynamic buckling of a laminated composite stringer-stiffened cylindrical panel. *Composites Part B: Engineering* 43(5): 2348–2358.
- Mustafa BAJ and Ali R (1989). An energy method for free vibration analysis of stiffened circular cylindrical shells. *Computers & Structures* 32(2): 355–363.

- Qu Y, Wu S, Chen Y and Hua H (2013). Vibration analysis of ring-stiffened conical-cylindrical-spherical shells based on a modified variational approach. *International Journal of Mechanical Sciences* 69: 72–84.
- Ren M, Li T, Huang Q and Wang B (2014). Numerical investigation into the buckling behavior of advanced grid stiffened composite cylindrical shell. *Journal of Reinforced Plastics and Composites* 33(16): 1508–1519.
- Sadeghifar M, Bagheri M and Jafari AA (2011). Buckling analysis of stringer-stiffened laminated cylindrical shells with nonuniform eccentricity. *Archive of Applied Mechanics* 81(7): 875–886.
- Semenov A (2021). Buckling of Shell Panels Made of Fiberglass and Reinforced with an Orthogonal Grid of Stiffeners. *Journal of Applied and Computational Mechanics* 7(3): 1856–1861.
- Semenov AA (2016). Strength and stability of geometrically nonlinear orthotropic shell structures. *Thin-Walled Structures* 106: 428–436.
- Solovei NA, Krivenko OP and Malygina OA (2015). Finite element models for the analysis of nonlinear deformation of shells stepwise-variable thickness with holes, channels and cavities. *Magazine of Civil Engineering* (1(53)): 56–69.
- Srinivasan RS and Krishnan PA (1989). Dynamic analysis of stiffened conical shell panels. *Computers & Structures* 33(3): 831–837.
- Sun Y, Qiu Y and Wu Y (2013). Modeling of Wind Pressure Spectra on Spherical Domes. *International Journal of Space Structures* 28(2): 87–100.
- Talebitooti M, Ghayour M, Ziaei-Rad S and Talebitooti R (2010). Free vibrations of rotating composite conical shells with stringer and ring stiffeners. *Archive of Applied Mechanics* 80(3): 201–215.
- Totaro G (2016). Flexural, torsional, and axial global stiffness properties of anisogrid lattice conical shells in composite material. *Composite Structures* 153: 738–745.
- Tu TM and Loi NV (2016) Vibration Analysis of Rotating Functionally Graded Cylindrical Shells with Orthogonal Stiffeners. *Latin American Journal of Solids and Structures* 13(15): 2952–2969.
- Uematsu Y, Kuribara O, Yamada M, Sasaki A and Hongo T (2001). Wind-induced dynamic behavior and its load estimation of a single-layer latticed dome with a long span. *Journal of Wind Engineering and Industrial Aerodynamics* 89(14–15): 1671–1687.
- Verwimp E, Tysmans T, Mollaert M and Berg S (2015). Experimental and numerical buckling analysis of a thin TRC dome. *Thin-Walled Structures* 94: 89–97.
- Wang B, Tian K, Hao P, Zheng Y, Ma Y and Wang J (2016). Numerical-based smeared stiffener method for global buckling analysis of grid-stiffened composite cylindrical shells. *Composite Structures* 152: 807–815.
- Wang CM, Swaddiwudhipong S and Tian J (1997). Ritz Method for Vibration Analysis of Cylindrical Shells with Ring Stiffeners. *Journal of Engineering Mechanics* 123(2): 134–142.
- Wang JT-S and Hsu T-M (1985). Discrete analysis of stiffened composite cylindrical shells. *AIAA Journal* 23(11): 1753–1761.
- Wang X (2007). Nonlinear stability analysis of thin doubly curved orthotropic shallow shells by the differential quadrature method. *Computer Methods in Applied Mechanics and Engineering* 196(17–20): 2242–2251.
- Yu W and Li ZL (2016). Structural Similitude for Prestressed Vibration and Buckling of Eccentrically Stiffened Circular Cylindrical Panels and Shells by Energy Approach. *International Journal of Structural Stability and Dynamics* 16(10): 1550074.
- Zhao X, Liew KM and Ng TY (2002). Vibrations of rotating cross-ply laminated circular cylindrical shells with stringer and ring stiffeners. *International Journal of Solids and Structures* 39(2): 529–545.